

# Synchronous Tunneling in a Multidimensional Quartic Potential: Competing Instanton Pathways and $D_4$ Symmetry Melting

Pervez Hoodbhoy,<sup>a)</sup> M. Haashir Ismail, and M. Mufassir

*The Black Hole, Sector G-11/3, Islamabad, Pakistan*

(Dated: 12 May 2026)

Semi-classical analysis is used to investigate synchronous quantum tunneling in a multidimensional potential energy surface (PES) characterized by four degenerate minima, serving as a foundational model for coupled vibrational modes. The primary challenge in such systems is the non-linear “locking” of trajectories where degrees of freedom must traverse their respective barriers synchronously. Starting from the Feynman path integral in imaginary time, we analytically identify longitudinal, transverse, and diagonal instanton configurations that mediate competing tunneling pathways between minima. The translational zero mode for each trajectory is treated rigorously by transforming to a comoving rotating frame. By applying the Gelfand-Yaglom method to the functional determinant and utilizing graph theory to sum the multi-flavor dilute instanton gas, we derive coherent Rabi-type oscillations and exact ground-state tunneling splittings. Crucially, we identify a critical coupling regime where the discrete  $D_4$  spatial symmetry of the minima undergoes a topological ‘melting’ transition into a continuous  $O(2)$  rotational symmetry. These analytical results, validated against high-precision numerical diagonalization, provide a rigorous benchmark for multidimensional computational techniques, such as Ring Polymer Instanton (RPI) theory, particularly in the strongly coupled regime where standard discrete instanton approximations break down.

PACS numbers: 03.65.Sq, 82.20.Xr, 31.15.xg

Keywords: multidimensional tunneling, instanton theory, semiclassical analysis, symmetry melting, functional determinants, coupled vibrational modes

---

<sup>a)</sup>Electronic mail: hoodbhoy@mit.edu

## I. INTRODUCTION

Quantum tunneling across multidimensional potential energy surfaces (PES) is a cornerstone of modern chemical physics, dictating reaction rates, kinetic isotope effects, and vibrational tunneling splittings in complex molecular systems. While the canonical double-well potential provides a paradigmatic starting point for a single degree of freedom (DOF), real molecular tunneling—such as the synchronous rearrangement of hydrogen bonds in water clusters or the inversion of symmetric molecules—is a collective, multi-DOF process. To tackle these high-dimensional PES landscapes, the chemical physics community relies heavily on computational semi-classical methods, most notably Ring Polymer Instanton (RPI) theory pioneered by Richardson and others<sup>1-4</sup>. Using instantons, Kryvohuz<sup>6</sup> computed reaction rate constants in multidimensional chemical systems. Erakovic et.al.<sup>7</sup> derive a multidimensional instanton theory that accommodates general, asymmetric paths and apply it to the vibrational splittings of water dimers and trimers. Using a potential that maps identically into the one used in this paper, Benderskii et.al.<sup>8</sup> identify competing tunneling trajectories in a two-dimensional potential with variable topology as a model for quantum bifurcations. Various path integral approximations to quantum dynamics have been reviewed by Althorpe<sup>9</sup>.

RPI and related multidimensional instanton approaches successfully discretize the imaginary-time path integral to locate optimal tunneling pathways (first-order saddle points) without solving the exact multidimensional Schrödinger equation. However, because these methods are primarily numerical, they provide limited analytical insight into the underlying tunneling mechanisms. Furthermore, numerical steepest-descent approximations often obscure the complex mathematical boundary where competing tunneling trajectories interact or where the discrete nature of the minima begins to break down under strong coupling.

To bridge this gap between numerical computation and analytical rigor, in this paper we investigate a highly symmetric, coupled multi-DOF quartic potential. As demonstrated in Appendix B, such a potential emerges naturally when modeling the composite tunneling of a 1D “diatomic molecule.” While seemingly simple, extracting the exact Feynman amplitude for this system is actually a formidable analytical challenge due to the non-linear “locking” of trajectories. In a composite system, tunneling is not a solitary event; energy conservation dictates that coupled fields must initiate and terminate their motion simultaneously,

concentrating their combined energy within a localized temporal window.

The central theoretical challenge in analytically solving such a multi-DOF system lies in the treatment of the zero mode and the evaluation of the fluctuation determinant. In computational approaches such as RPI, this is quite simply handled. The continuous imaginary-time periodic orbit (bounce) responsible for tunneling splittings is discretized into a finite necklace of  $N$  beads. The zero-mode is then managed by factoring out the cyclic permutation of these beads. In contrast, our approach maintains the continuous nature of the periodic orbits, obtained by solving the coupled classical equations of motion. By transforming the system into a comoving rotating frame that tracks the classical instanton trajectory, we successfully isolate the longitudinal, “force-free” tunneling direction from the transverse fluctuations subject to curvature-induced restoring forces. This explicit treatment of Coriolis and velocity-dependent fictitious forces allows us to perform the Gaussian integrations perturbatively. The functional determinant thus obtained is evaluated using the Gelfand-Yaglom method. As the final step, the dilute instanton gas approximation is generalized using a graph-theoretic  $K_4$  summation to account for competing multi-flavor (longitudinal, transverse, and diagonal) instanton configurations. This allows us to derive closed-form expressions for the coherent Rabi-type oscillations and the energy splittings of the four lowest-lying states. We validate these analytical results against high-precision numerical diagonalization, finding excellent agreement in the deep semi-classical limit.

Crucially, our analytical derivation of the pre-factor reveals phenomena that are difficult to isolate in purely numerical frameworks. At strong coupling, the pre-factor develops an essential singularity that totally overwhelms the exponential suppression factor. At this critical point, the discrete  $D_4$  spatial symmetry of the four-well system experiences a catastrophic breakdown, “melting” into a continuous  $O(2)$  rotational symmetry. This unphysical divergence acts as a theoretical red flag, signifying a phase transition from discrete quantum tunneling to continuous zero-point rotation. Such exact analytical benchmarks are critical for the chemical physics community, as they precisely identify the topological limits where standard discrete instanton approximations must inevitably break down.

In the final section of this paper we shall compare our work with that in the chemical physics literature where semi-classical methods have been used to compute energy splittings, reaction rates, and where the possibility of multiple pathways has been investigated.

## II. COUPLED INSTANTONS MODEL

The holy grail of all tunneling calculations is to find the Feynman amplitude in imaginary (or Euclidean) time  $t$ ,

$$\mathcal{A}_{if} = \langle f, T/2 | e^{-\frac{Ht}{\hbar}} | i, -T/2 \rangle = \mathcal{N} \int [dx(t)] e^{-\frac{S[x]}{\hbar}}, \quad (1)$$

where  $S[x]$  is the Euclidean action and in the finite temperature case  $\hbar^{-1}$  is replaced with  $kT$ . The system is in its initial state at time  $t = -T/2$  and makes its way to the final state at  $t = T/2$  by traveling on all possible paths connecting the initial to the final state. To get bound state energies and wavefunctions one eventually takes  $T \rightarrow \infty$ . In the semiclassical approximation, fluctuations away from these paths are allowed up to the quadratic level while the rest can be treated in a perturbative expansion. Building on the techniques developed in the foundational works of instanton theory<sup>10–12</sup> (a recent review<sup>13</sup> is particularly useful), in this paper we shall investigate the system defined by the Euclidean Lagrangian,

$$L = \frac{1}{2}m_p \left( \frac{dx}{dt} \right)^2 + \frac{1}{2}m_q \left( \frac{dy}{dt} \right)^2 + V(x, y)$$

$$V(x, y) = \frac{m_p \omega_p^2}{8x_p^2} (x^2 - x_p^2)^2 + \frac{m_q \omega_q^2}{8y_q^2} (y^2 - y_q^2)^2 + c_{pq} (x^2 - x_p^2)(y^2 - y_q^2). \quad (2)$$

Standard notation has been used to represent two symmetric double wells with minima at  $x_p, y_q$  coupled together with strength  $c_{pq}$ . We make the following re-definitions:

$$p = \frac{x}{x_p}, \quad q = \frac{y}{y_p}, \quad a_p = \frac{m_p x_p^2}{\hbar}, \quad b_p = \frac{m_p x_p^2 \omega_p^2}{\hbar}, \quad a_q = \frac{m_q y_q^2}{\hbar}, \quad b_q = \frac{m_q y_q^2 \omega_q^2}{\hbar}. \quad (3)$$

To be kept in mind is the smallness of  $\hbar$ ; this is key to the semi-classical method's success. The five independent constants  $a_p, b_p, a_q, b_q, c$  are set by some underlying physical model. The particular form of interaction is, as we show in Appendix B, of interest in at least one physical problem but, apart from the tunneling of a composite system of particles, other optical or condensed matter systems could also have such an effective potential. The system is defined by the (dimensionless) action  $S$ ,

$$S \equiv \frac{\mathbf{S}}{\hbar} = \int \mathcal{L} dt, \quad \mathcal{L} = \frac{1}{2}a_p \dot{p}^2 + \frac{1}{2}a_q \dot{q}^2 + V(p, q),$$

$$V(p, q) = \frac{1}{8}b_p (p^2 - 1)^2 + \frac{1}{8}b_q (q^2 - 1)^2 + \frac{1}{4}c (p^2 - 1)(q^2 - 1). \quad (4)$$

$V(p, q)$  is shown schematically in Fig. 1.

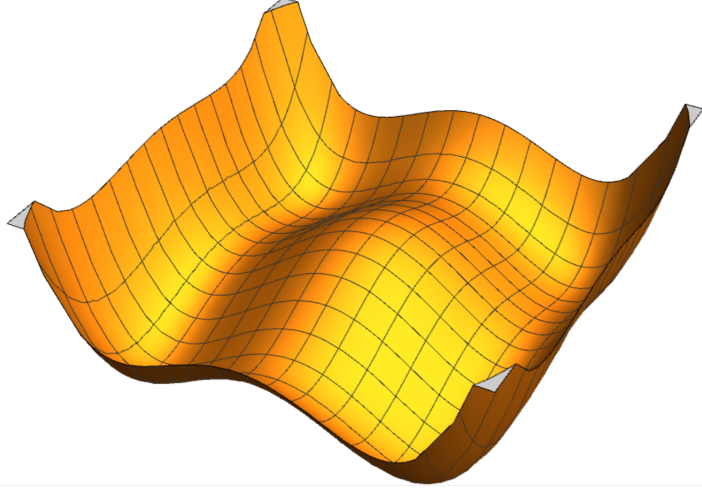


FIG. 1. Schematic of the four-well symmetric quartic potential  $V(p, q)$  for parameters  $b_p = 2, b_q = 1$ , and  $c = 1/2$ . The four degenerate minima at  $(\pm 1, \pm 1)$  are separated by saddle points, facilitating multiple distinct tunneling pathways.

Consider now two instantons corresponding to two different physical variables interacting with each other through  $V(p, q)$ . Let us first explore the parts of parameter space relevant to the tunneling problem at hand. All masses and spring constants are taken positive definite, i.e.  $a_p > 0, b_p > 0, a_q > 0, b_q > 0$ . Further, the minima  $x_p, y_q$  must satisfy  $x_p^2 > 0, y_q^2 > 0$ . With  $P = p^2 - 1$  and  $Q = q^2 - 1$  we may rewrite the potential in Eq. 4,

$$V(p, q) = \frac{1}{8}b_p P^2 + \frac{1}{8}b_q Q^2 + \frac{1}{4}cPQ = \frac{1}{8}b_p \left( P + \frac{c}{b_p}Q \right)^2 + \frac{\Delta}{8b_p}Q^2. \quad (5)$$

If the discriminant  $\Delta = b_p b_q - c^2 > 0$ , then  $V \geq 0$ . The critical points of  $V$  are at  $A = (\pm 1, \pm 1), B = (0, q)$ , and  $C = (p, 0)$ . To ascertain the behaviour of  $V$  we must examine the Hessian matrix  $H(p, q)$  at all such points. At  $A$ ,  $V(A) = 0$  and  $\det[H(A)] = 4\Delta > 0$ . Hence the four  $A$  points are indeed true local minima. At points  $B$ ,

$$V(0, q) = \frac{1}{8}b_p + \frac{1}{8}b_q Q^2 - \frac{1}{4}cQ = \frac{1}{8}b_q \left( Q - \frac{c}{b_q} \right)^2 + \frac{\Delta}{8b_q}. \quad (6)$$

This will take its minimum value  $\Delta/(8b_q) > 0$  when  $Q_m = c/b_q$  i.e. when  $q_m^2 = 1 + c/b_q$ . At this point  $\det[H(0, q_m)] = -(1 + c/b_q)\Delta$ . This will be a saddle point if  $b_q + c > 0$ . The conclusion for all points  $C$  is similar. In summary, to have exactly four degenerate minima and no other local minimum, requires:

$$b_p b_q > c^2, \quad b_p + c > 0, \quad b_q + c > 0. \quad (7)$$

While  $V$  is unbounded above in the  $R_2$  plane, a local maximum at the origin,

$$V(0,0) = \frac{1}{8}b_p + \frac{1}{8}b_q + \frac{1}{4}c, \quad (8)$$

is guaranteed because  $\det[H(0,0)] \sim (b_p + c)(b_q + c) > 0$  as per Eq. 7. Let us now consider the interaction between the  $p$  and  $q$  fields. This operates only for times when  $p^2 \neq 1$  and  $q^2 \neq 1$  and then rapidly turns itself off. For  $c = 0$  two decoupled instantons mediate between their respective vacuum states at  $p = \pm 1$  and  $q = \pm 1$ .

As per the semi-classical prescription, the action  $S[p, q]$  in Eq. 4 must be expanded in a functional Taylor series around the classical path up to and including quadratic terms,  $S = S_0 + S_1 + S_2 + \dots$ . What remains can be treated perturbatively.

$$S[p, q] = S[p_c, q_c] + \int dt' \left[ \frac{\delta S}{\delta p} \eta + \frac{\delta S}{\delta q} \xi \right] + \frac{1}{2} \int dt' dt'' \left[ \frac{\delta^2 S}{\delta p \delta p} \eta \eta + \frac{\delta^2 S}{\delta q \delta q} \xi \xi + 2 \frac{\delta^2 S}{\delta p \delta q} \eta \xi + \dots \right] \quad (9)$$

The partial derivatives indicated above must be evaluated at  $p = p_c, q = q_c$ . Deviations from the classical path  $\eta(t) = p - p_c$  and  $\xi(t) = q - q_c$  are integrated over subject to the end point conditions,  $\eta(-T/2) = \eta(T/2) = \xi(-T/2) = \xi(T/2) = 0$ . Some algebra gives the order by order decomposition of the dimensionless action,

$$\begin{aligned} S_0 &= \frac{1}{2} \int dt \left[ a_p \dot{p}_c^2 + \frac{1}{4} b_p (p_c^2 - 1)^2 + a_q \dot{q}_c^2 + \frac{1}{4} b_q (q_c^2 - 1)^2 + \frac{1}{2} c (p_c^2 - 1)(q_c^2 - 1) \right], \\ S_1 &= \int dt \left[ a_p \dot{p}_c \dot{\eta} + \frac{b_p}{2} p_c (p_c^2 - 1) \eta + \frac{c}{2} p_c (q_c^2 - 1) \eta + a_q \dot{q}_c \dot{\xi} + \frac{b_q}{2} q_c (q_c^2 - 1) \xi + \frac{c}{2} q_c (p_c^2 - 1) \xi \right], \\ S_2 &= \frac{1}{2} \int dt \left[ a_p \dot{\eta}^2 + \frac{b_p}{2} (3p_c^2 - 1) \eta^2 + \frac{c}{2} (q_c^2 - 1) \eta^2 + a_q \dot{\xi}^2 + \frac{b_q}{2} (3q_c^2 - 1) \xi^2 \right. \\ &\quad \left. + \frac{c}{2} (p_c^2 - 1) \xi^2 + 2c p_c q_c \eta \xi \right], \\ &\equiv \frac{1}{2} \int dt \Omega^T \mathcal{M} \Omega. \end{aligned} \quad (10)$$

The fluctuation vector  $\Omega$  is defined as,

$$\Omega = \begin{bmatrix} \eta(t) \\ \xi(t) \end{bmatrix}, \quad \mathcal{M} = AM_D + M', \quad A = \begin{bmatrix} a_p & 0 \\ 0 & a_q \end{bmatrix}. \quad (11)$$

$M_D, M'$  are differential operators which are hermitian since the functions on which they

operate vanish at the boundaries,

$$M_D = \begin{bmatrix} M_{pp} & 0 \\ 0 & M_{qq} \end{bmatrix}, \quad M' = \begin{bmatrix} 0 & M_{pq} \\ M_{qp} & 0 \end{bmatrix}, \quad (12)$$

$$M_{pp} = -\frac{d^2}{dt^2} + V_{pp}, \quad M_{qq} = -\frac{d^2}{dt^2} + V_{qq}, \quad M_{pq} = M_{qp} = V_{pq}. \quad (13)$$

The elements of the Hessian matrix  $V_{pp}, V_{qq}, V_{pq}$  and the dimensionless couplings  $\mu, \nu$  are defined below:

$$V_{pp} = \frac{\omega_p^2}{2}(3p_c^2 - 1) + \mu\omega_p^2(q_c^2 - 1), \quad V_{qq} = \frac{\omega_q^2}{2}(3q_c^2 - 1) + \nu\omega_q^2(p_c^2 - 1), \\ V_{pq} = V_{qp} = cp_cq_c, \quad \text{where } \mu = \frac{c}{2b_p}, \quad \nu = \frac{c}{2b_q}. \quad (14)$$

From the definitions in Eq. 3 we have  $\omega_p^2 = b_p/a_p$  and  $\omega_q^2 = b_q/a_q$ . The requirement  $S_1 = 0$ , then yields the coupled Euler-Lagrange equations for  $p_c$  and  $q_c$ ,

$$\frac{d^2 p_c}{dt^2} = \omega_p^2 \left[ \frac{1}{2}(p_c^2 - 1) + \mu(q_c^2 - 1) \right] p_c, \quad \frac{d^2 q_c}{dt^2} = \omega_q^2 \left[ \frac{1}{2}(q_c^2 - 1) + \nu(p_c^2 - 1) \right] q_c. \quad (15)$$

Insight into this system can be obtained by noting that the classical Euclidean energy  $E \equiv -T + V$  is conserved at the classical (but not quantum) level. Since the kinetic energy in imaginary time is negative,  $E$  becomes:

$$E = -\frac{1}{2}a_p\dot{p}_c^2 - \frac{1}{2}a_q\dot{q}_c^2 + \frac{1}{8}b_p(p_c^2 - 1)^2 + \frac{1}{8}b_q(q_c^2 - 1)^2 + \frac{1}{4}c(p_c^2 - 1)(q_c^2 - 1). \quad (16)$$

We may now take the derivative and use the EOM's to conclude that  $E$  is a constant of motion,

$$\frac{dE}{dt} = 0. \quad (17)$$

Since  $\dot{p}_c = 0, \dot{q}_c = 0$  when  $p, q$  are perched at a hilltop, the kinetic and potential energies both vanish there and so one may choose  $E = 0$ . Integrating both sides of Eq. 16 and then inserting into Eq. 10 yields,

$$S_0 = \int_{-\frac{\tau}{2}}^{\frac{\tau}{2}} dt [a_p\dot{p}_c^2(t) + a_q\dot{q}_c^2(t)] = S_{0p} + S_{0q}, \quad \text{where } S_{0p} \equiv a_p\|\dot{p}_c\|^2, \quad S_{0q} \equiv a_q\|\dot{q}_c\|^2. \quad (18)$$

The  $L_2$  norms used above are defined in the standard way,

$$\|f\|^2 = \int_{-\frac{\tau}{2}}^{\frac{\tau}{2}} dt f^*(t)f(t). \quad (19)$$

Energy conservation holds because there is no explicit dependence on time  $t$  in the potential  $V(p, q)$  in Eq. 4. Along this path the action stays constant, i.e. unless  $c = 0$  there is a single collective coordinate or single zero eigenvalue mode.

### III. THE ZERO MODE

For uncoupled instantons each instanton has its own zero mode but even the slightest coupling between them results in collapse to a single mode. Let us extend the textbook analysis to two coupled instantons. This, as we shall see, is far from trivial. In fact we shall be able to achieve an analytic solution only for special cases. To obtain the eigenfunction for the soft direction, consider solutions  $p_c, q_c$  of the EOM for displaced solutions,  $p_c(t, t_c), q_c(t, t_c)$  centred at  $t = t_c$ . This origin is arbitrary and so shifting it by any amount leaves the action unchanged. Suppose the shift is by an infinitesimal amount  $\delta t_c$ , i.e.  $t_c \rightarrow t_c + \delta t_c$ . Then,

$$S[p_c(t, t_c + \delta t_c), q_c(t, t_c + \delta t_c)] = S[p_c(t, t_c), q_c(t, t_c)] \quad (20)$$

Using the chain rule, the above condition can be expanded out:

$$\begin{aligned} 0 = & \delta t_c \int dt \left[ \frac{\delta S}{\delta p_c(t)} \dot{p}_c(t) + \frac{\delta S}{\delta q_c(t)} \dot{q}_c(t) \right] \\ & + \frac{\delta t_c^2}{2} \iint dt dt' \left[ \dot{p}_c(t) \frac{\delta^2 S}{\delta p_c(t) \delta p_c(t')} \dot{p}_c(t') + \dot{q}_c(t) \frac{\delta^2 S}{\delta q_c(t) \delta q_c(t')} \dot{q}_c(t') \right. \\ & \left. + 2\dot{p}_c(t) \frac{\delta^2 S}{\delta p_c(t) \delta q_c(t')} \dot{q}_c(t') \right] \end{aligned} \quad (21)$$

The first term on the RHS above is zero because the first order variations have been required to vanish. The second-order term represents the energy cost of shifting the ‘‘center’’  $t_c$  of the instanton solution. Because the action is invariant under a global time translation  $t \rightarrow t + \delta t_c$ , the total first and second-order variations with respect to  $t_c$  are zero. Eq. 21, expressed in terms of  $\mathcal{M}$  and  $\dot{\Phi}_c$ , is

$$\mathcal{M} \dot{\Phi}_c(t) = 0, \quad \dot{\Phi}_c \equiv \begin{bmatrix} \dot{p}_c(t) \\ \dot{q}_c(t) \end{bmatrix}. \quad (22)$$

Thus  $\dot{\Phi}_c(t)$  is the (unnormalized) zero mode of the two instanton system. This can be reconfirmed by differentiating the EOM’s in Eqs. 15. The structure of  $\mathcal{M}$  above suggests that we consider the generalized eigenvalue problem with  $(\mathcal{M}, A)$  as the matrix ‘pencil’,  $\mathcal{M} \Phi_n = \lambda_n A \Phi_n$ , which leads to the normalization condition  $\int dt \Phi_n^T A \Phi_m(t) = \delta_{nm}$ .

### IV. L-T DECOMPOSITION

The coupled differential equations Eqs. 15 define a path in  $(p, q)$  space akin to motion along the bottom of a valley that twists and turns from start to finish. The fact that

$\mathcal{M}\dot{\Phi}_c(t) = 0$  tells us physically that at every point on the instanton's trajectory there is a soft direction; along it a fluctuation can propagate freely whereas to travel perpendicularly requires it to work against a restoring force. Intuitively, stability is assured if there is stiffness against a transverse perturbation. With this in mind, let us define a frame (see Fig.2) comoving with the instanton and perform an instantaneous, time dependent rotation by  $\theta$  with  $\theta(t)$  chosen so that the longitudinal axis lies along the soft direction,

$$R = \begin{bmatrix} \cos \theta & -\sin \theta \\ \sin \theta & \cos \theta \end{bmatrix}, \quad \tan \theta = \frac{\dot{q}_c}{\dot{p}_c}. \quad (23)$$

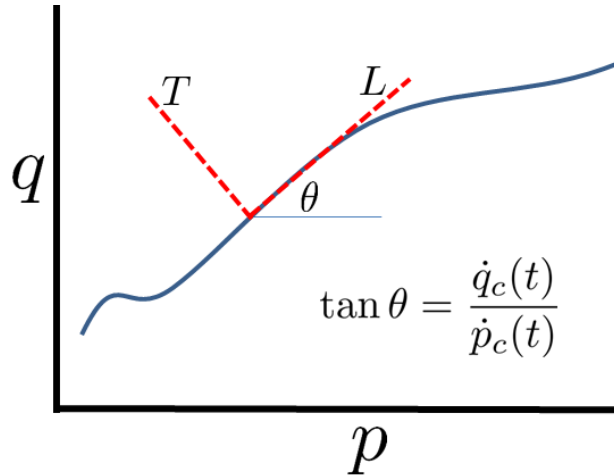


FIG. 2. Decomposition of the fluctuation matrix  $\mathcal{M}$  in the frame comoving with the instanton. The longitudinal axis  $L$  represents the soft direction associated with the translational zero mode, while the transverse axis  $T$  tracks fluctuations subject to the curvature-induced restoring forces and non-inertial effects in the rotating frame.

With  $\mathcal{M} \rightarrow \mathcal{M}_{rot} = R^T \mathcal{M} R$ , after some considerable algebra we obtain its components in the rotated frame:

$$\mathcal{M}_{rot} = \begin{bmatrix} \mathcal{M}_L & \mathcal{M}_{LT} \\ \mathcal{M}_{TL} & \mathcal{M}_T \end{bmatrix}, \quad (24)$$

where,

$$\begin{aligned}
\mathcal{M}_L &= \frac{1}{v^2} \left[ (a_p \dot{p}_c^2 + a_q \dot{q}_c^2) \hat{K} + (a_p - a_q) \dot{p}_c \dot{q}_c (2\dot{\theta} \partial_t + \ddot{\theta}) + a_p \dot{p}_c^2 V_{pp} + a_q \dot{q}_c^2 V_{qq} + 2\dot{p}_c \dot{q}_c V_{pq} \right] \\
\mathcal{M}_T &= \frac{1}{v^2} \left[ (a_p \dot{q}_c^2 + a_q \dot{p}_c^2) \hat{K} - (a_p - a_q) \dot{p}_c \dot{q}_c (2\dot{\theta} \partial_t + \ddot{\theta}) + a_p \dot{q}_c^2 V_{pp} + a_q \dot{p}_c^2 V_{qq} - 2\dot{p}_c \dot{q}_c V_{pq} \right] \\
\mathcal{M}_{LT} &= \frac{1}{v^2} \left[ -(a_p - a_q) \dot{p}_c \dot{q}_c \hat{K} + (a_p \dot{p}_c^2 + a_q \dot{q}_c^2) (2\dot{\theta} \partial_t + \ddot{\theta}) + \dot{p}_c \dot{q}_c (a_q V_{qq} - a_p V_{pp}) + (\dot{p}_c^2 - \dot{q}_c^2) V_{pq} \right] \\
\mathcal{M}_{TL} &= \frac{1}{v^2} \left[ -(a_p - a_q) \dot{p}_c \dot{q}_c \hat{K} - (a_p \dot{q}_c^2 + a_q \dot{p}_c^2) (2\dot{\theta} \partial_t + \ddot{\theta}) + \dot{p}_c \dot{q}_c (a_q V_{qq} - a_p V_{pp}) + (\dot{p}_c^2 - \dot{q}_c^2) V_{pq} \right]
\end{aligned} \tag{25}$$

The auxiliary quantities are defined as,

$$\hat{K} = -\frac{d^2}{dt^2} + \dot{\theta}^2, \quad v^2 = \dot{p}_c^2 + \dot{q}_c^2. \tag{26}$$

Because  $\mathcal{M}$  contains the operator  $\frac{d^2}{dt^2}$ , the time-dependence of  $R(t)$  has generated non-inertial terms:  $2\dot{\theta} \frac{d}{dt}$ , the Euler term  $\ddot{\theta}$ , and the centrifugal term,  $\dot{\theta}^2$ . Note that although  $\mathcal{M}$  is symmetric,  $\mathcal{M}_{rot}$  is not - a consequence of fictitious forces in the rotating frame. In geometric terms, for any parameterized curve, the curvature of a path  $\Phi_c(t) = (p_c(t), q_c(t))$  in the  $p$ - $q$  plane is given by the kinematic formula:

$$\kappa(t) = \frac{|\dot{p}_c \ddot{q}_c - \dot{q}_c \ddot{p}_c|}{(\dot{p}_c^2 + \dot{q}_c^2)^{3/2}}. \tag{27}$$

From the relationship  $\tan \theta = \dot{q}_c / \dot{p}_c$ , the time derivative of the angle is:

$$\dot{\theta} = \frac{\dot{p}_c \ddot{q}_c - \dot{q}_c \ddot{p}_c}{\dot{p}_c^2 + \dot{q}_c^2} = \kappa(t) \sqrt{\dot{p}_c^2 + \dot{q}_c^2} = \kappa(t) v. \tag{28}$$

## V. SOLUTION OF EOM'S

The coupled equations of motion Eqs. 15 which lead to the classical solutions  $p_c(t), q_c(t)$ , must now be tackled. Various cases are distinguished by the different imposed boundary conditions. The null solution  $p_c^2(t) = 1, q_c^2(t) = 1$  satisfies the EOM's with zero action,  $S_{0p} = S_{0q} = 0$ . For non-zero action, the solutions fall into 3 types which we shall call  $P, Q, R$  as below:

$$\mathbf{P}: p_c(\mp\infty) = \mp 1, q_c(\mp\infty) = 1 \tag{29}$$

$$\mathbf{Q}: p_c(\mp\infty) = 1, q_c(\mp\infty) = \mp 1 \tag{30}$$

$$\mathbf{R}: p_c(\mp\infty) = \mp 1, q_c(\mp\infty) = \mp 1 \tag{31}$$

These are illustrated in Fig. 3.

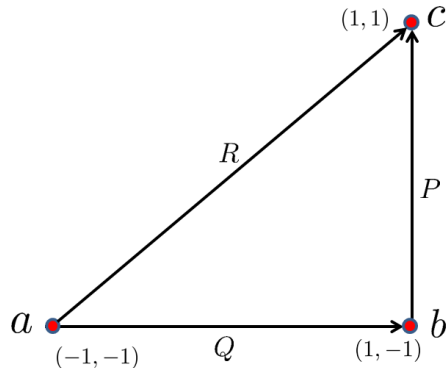


FIG. 3. The three primary instanton configurations in  $(p, q)$  space: the edge instantons  $P$  and  $Q$ , which involve a single field transition, and the diagonal  $R$  instanton, representing synchronous tunneling of both degrees of freedom.

So far our treatment has been both exact and general. But solving the coupled non-linear system is a daunting task. Let us therefore consider the case where both systems have identical parameters. We define the dimensionless quantity  $\lambda$ ,

$$\lambda = \frac{m\omega L^2}{\hbar}, \quad (32)$$

which will serve as the large parameter of the theory and thus is effectively  $\hbar^{-1}$ . The system parameters are re-expressed as,

$$\omega_p = \omega_q = \omega, \quad a_p = a_q, \quad \mu = \nu. \quad (33)$$

With  $\tau = \omega t$  as the dimensionless time (henceforth a dot will always denote the derivative with respect to  $\tau$ ), the action takes on a pleasingly simple form,

$$S = \frac{\lambda}{2} \int d\tau \left[ \dot{p}^2 + \dot{q}^2 + \frac{1}{4}(p^2 - 1)^2 + \frac{1}{4}(q^2 - 1)^2 + \mu(p^2 - 1)(q^2 - 1) \right]. \quad (34)$$

The EOM's are symmetrical:

$$\ddot{p}_c = \left[ \frac{1}{2}(p_c^2 - 1) + \mu(q_c^2 - 1) \right] p_c, \quad \ddot{q}_c = \left[ \frac{1}{2}(q_c^2 - 1) + \mu(p_c^2 - 1) \right] q_c, \quad (35)$$

and cry out for a symmetrical solution.

**R case:** As the Euclidean times goes from  $-\infty$  to  $\infty$ , both  $p, q$  move together diagonally

from  $a$  to  $c$  in the form of a single energy lump. The solution of the EOM's Eq. 35, takes the standard tanh form:

$$p_c = q_c = \tanh \frac{\omega_+ \tau}{2}, \quad \omega_+ = \sqrt{1 + 2\mu}. \quad (36)$$

From Eq. 18 the corresponding action is computed to be,

$$S_0^R = \frac{4}{3} \lambda \omega_+. \quad (37)$$

Let us verify that for  $p = q$  this is globally the absolute minimum value of the action functional Eq. 4 and satisfies the BPS Saturation (Bogomol'nyi Completion) condition for the given boundary conditions,  $p(\mp\infty) = \mp 1$ . To this end, rewrite the (dimensionless) action with  $p$  and  $q$  set equal to each other,

$$S = \lambda \int_{-\infty}^{\infty} d\tau \left[ \dot{p}^2 + \left( \frac{1}{4} + \frac{1}{2}\mu \right) (1 - p^2)^2 \right] = \lambda \int_{-\infty}^{\infty} d\tau \left( \dot{p} - \frac{1}{2}\omega_+(1 - p^2) \right)^2 + S_{top}. \quad (38)$$

The first term is non-negative and is zero only when the first-order BPS equation is satisfied:

$$\dot{p} = \frac{1}{2}\omega_+(1 - p^2). \quad (39)$$

This leaves only  $S_{top}$ , the topological term defined as,

$$S_{top} = \lambda \int_{-\infty}^{\infty} d\tau \dot{p}(1 - p^2). \quad (40)$$

The resulting trajectory is  $p_c = \tanh \omega_+ \tau / 2$  as in Eq. 37.  $S_{top}$ , whose value is  $S_0^R$  as in Eq. 37, solely determines the action. Further, any path where  $p(\tau) \neq q(\tau)$  introduces a non-zero difference field  $v(t) = (p - q) / \sqrt{2}$ . The action functional  $S[p, q]$  is minimized when the transverse fluctuations  $v(t)$  are zero because the coupling  $\mu$  creates a potential valley along the  $p = q$  diagonal. Hence  $S[p \neq q] > S[p = q]$ . We have belabored this point here because, as will be seen later, this enters critically into calculating the functional determinant.

**P,Q cases:** This corresponds to the  $p$  instanton transiting to the other peak with  $q$  being dragged along by it but, eventually, returning to its starting position i.e.  $p_c(\mp\infty) = \mp 1$ ,  $q_c(\mp\infty) = -1$ . Unfortunately, unlike the  $R$  case, no exact solution seems possible and so we must look for a perturbative solution valid for small  $\mu$  values,

$$p_c(\tau) = p_0 + \mu p_1 + \mu^2 p_2 + \dots, \quad q_c(\tau) = q_0 + \mu q_1 + \mu^2 q_2 + \dots \quad (41)$$

We start from the uncoupled state,

$$p_0 = \tanh \frac{\tau}{2}, \quad q_0 = -1. \quad (42)$$

This yields,

$$p_1 = 0, \text{ and, } \ddot{q}_1 - q_1 = (p_0^2 - 1)q_0 = \text{sech}^2 \frac{\tau}{2}. \quad (43)$$

The solution of equation for  $q_1$  is,

$$q_1 = 2 + 2\tau \sinh \tau - 4 \cosh \tau \ln \left( 2 \cosh \frac{\tau}{2} \right). \quad (44)$$

In physical terms,  $q_1(\tau)$  is the lump coupled to the  $p$  (driving) instanton. The source for  $p_2(\tau)$  is the interaction term  $2\mu q_0 q_1 p_0$ :

$$\left[ \frac{d^2}{d\tau^2} - \left( 1 - \frac{3}{2} \text{sech}^2 \frac{\tau}{2} \right) \right] p_2(\tau) = -2 \tanh \frac{\tau}{2} q_1(\tau). \quad (45)$$

An analytical solution for  $p_2(\tau)$  is also possible but is non-transparent, requiring a mix of hypergeometric functions. Instead, we display the plots of  $q_1(\tau)$  and  $p_2(\tau)$  in Fig. 4.

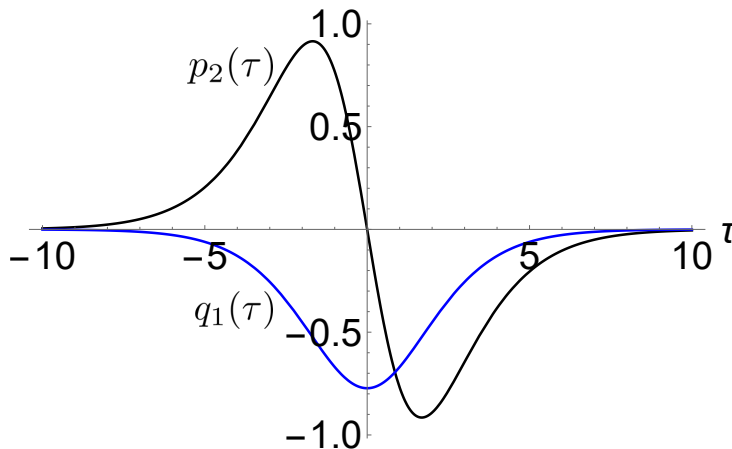


FIG. 4. Profiles of the auxiliary functions  $q_1(\tau)$  and  $p_2(\tau)$  used in the perturbative expansion of the edge instanton action. The function  $q_1(\tau)$  acts as the source for the  $p_2$  correction, illustrating the “dragging” effect of the secondary field during tunneling.

Fortunately, by manipulating the driving equation Eq. 45 for  $p_2$  only, we are able to get the kinetic energy to  $O(\mu^2)$  in a clean, analytical form,

$$\int_{-\infty}^{\infty} d\tau \dot{q}_c^2 = \mu^2 (4\pi^2 - 20 - 16\zeta(3)), \quad \int_{-\infty}^{\infty} d\tau \dot{p}_c^2 = \frac{2}{3} + 16\mu^2 \left[ 2 - \frac{\pi^2}{3} + \zeta(3) \right]. \quad (46)$$

This yields the action to second order,

$$S_0^P = S_0^Q = \frac{2}{3}\lambda(1 - 2(\pi^2 - 9)\mu^2 + \dots) \approx \frac{2}{3}\lambda(1 - 1.739\mu^2). \quad (47)$$

As can be seen from Fig. 4, the energy density of both  $p$  and  $q$  fields peaks at  $t = 0$  and rapidly dies away. Therefore this can be justifiably be called a 2-D instanton or kink.

To summarize this section: at the purely classical level, the amplitude for each path in  $(p, q)$  space that connects the initial vacuum to the final vacuum is weighted by the factor  $\exp(-S_0)$ . This dominates the tunneling amplitude. For the two specific paths explored, these factors (cf: Fig. 3) are:

- $a \rightarrow c$ :  $e^{-\frac{4}{3}\lambda\sqrt{1+2\mu}}$
- $a \rightarrow b$ :  $e^{-\frac{2}{3}\lambda(1-2(\pi^2-9)\mu^2)}$

For  $-0.5 < \mu < -0.45$  the diagonal path has lesser action (is preferred) in comparison to the indirect one which is mostly along the edges. We must keep in mind, however, that the exact location of the rightward limit is contingent on the validity of the small coupling expansion.

## VI. QUADRATIC FLUCTUATIONS

With solutions now in hand for the EOM's - exact for the  $R$  case and perturbative for the  $P, Q$  cases - we proceed to the next stage, i.e. the quadratic level fluctuations. These lead to the pre-factors multiplying the exponential of the action. For this we must first simplify the rotated matrix for the case of equal parameters.

**Diagonal Case:** The  $p, q$  instantons travel together along the diagonal  $\theta = \pi/4$  in  $p, q$  space with  $\dot{p}_c = \dot{q}_c$  and  $\dot{\theta} = \ddot{\theta} = 0$ . Having an exact solution vastly simplifies matters. Linear motion eliminates all non-inertial couplings and off-diagonal terms in  $\mathcal{M}_{rot}$ , Eq. 24. With  $p_c = q_c = \tanh \omega_+ \tau/2$ , the potentials are:

$$V_{pp} = V_{qq} = \frac{1}{2}(3p_c^2 - 1) + \mu(p_c^2 - 1), \quad V_{pq} = cp_c^2 = 2\mu p_c^2. \quad (48)$$

The rotated matrix  $\mathcal{M}_{rot}$  becomes exactly diagonal:

$$\mathcal{M}_{rot}^R = \lambda \begin{bmatrix} \mathcal{M}_L^R & 0 \\ 0 & \mathcal{M}_T^R \end{bmatrix}. \quad (49)$$

The longitudinal operator  $\mathcal{M}_L^R$ , and the transverse operator  $\mathcal{M}_T^R$ , reduce to:

$$\mathcal{M}_L^R = -\frac{d^2}{d\tau^2} + \omega_+^2 - \frac{3}{2}\omega_+^2 \operatorname{sech}^2 \frac{\omega_+\tau}{2}, \quad \mathcal{M}_T^R = -\frac{d^2}{d\tau^2} + \omega_-^2 - \left(\frac{3}{2} - \mu\right) \operatorname{sech}^2 \frac{\omega_+\tau}{2}. \quad (50)$$

In parallel with  $\omega_+$  we have defined  $\omega_-$  through  $\omega_{\pm} = 1 \pm 2\mu$ . As discussed in Appendix A, these are the scaled frequencies of the two independent oscillator modes that follow from diagonalizing the Hamiltonian near any of the four potential minima.

We next turn to stability issues. The eigenvalues of  $\mathcal{M}_L^R$  are strictly non-negative and so there are no runaway solutions; its stability is assured. The transverse operator  $\mathcal{M}_T^R$  demands closer inspection. At  $\mu = \frac{1}{2}$  the asymptotic potential height  $(1 - 2\mu)$  vanishes, and at  $\mu = -1/2$  the value of  $\omega_+$  is zero. For the eigenvalue problem  $\mathcal{M}_T^R \psi_n = \lambda_n \psi_n$ , a necessary condition for stability is that the lowest eigenvalue  $\lambda_0 > 0$ . On the other hand, the eigenvalues of the pure Pöschl-Teller part are known to be  $-\ell^2, -(\ell - 1)^2, \dots$ . Hence the lowest eigenvalue is  $\lambda_0 = k^2 - \ell^2$ . The range of  $\mu$  for which the solutions are stable is therefore  $-\frac{1}{2} < \mu < 0$ . Now take the critical case  $\mu = 0$  for which  $k = 2, \ell = 2$  and the transverse mode has a zero mode (marginal stability). There are two uncoupled instantons and thus two Goldstone modes, as indeed should be the case. Expanding for small  $\mu$ ,

$$\lambda_0 = \Omega^2 \left[ -\frac{4}{5}\mu + \frac{136}{125}\mu^2 \right] + \mathcal{O}(\mu^3). \quad (51)$$

This implies the following: for negative  $\mu$  (attractive interaction) the action is lowered and so  $p, q$  journey together as a localized energy packet. The potential well gets deeper as  $\mu$  becomes more negative. On the other hand, for a repulsive interaction, the solution of the EOM's is unstable and  $p, q$  journey separately. The bottom line: the diagonal instanton is a preferred path only for an attractive potential between  $p, q$  fields.

**Edge Case:** The rotation matrix  $\mathcal{M}_{rot}^P$  for the  $P, Q$  systems contains both velocity dependent diagonal as well as off-diagonal terms. The Coriolis terms make it non-symmetric.

$$\mathcal{M}_L^P = -\frac{d^2}{d\tau^2} + \dot{\theta}^2 + \frac{V_{pp}\dot{p}_c^2 + V_{qq}\dot{q}_c^2 + 4\mu V_{pq}\dot{p}_c\dot{q}_c}{\dot{p}_c^2 + \dot{q}_c^2} \quad (52)$$

$$\mathcal{M}_T^P = -\frac{d^2}{d\tau^2} + \dot{\theta}^2 + \frac{V_{pp}\dot{q}_c^2 + V_{qq}\dot{p}_c^2 - 4\mu V_{pq}\dot{p}_c\dot{q}_c}{\dot{p}_c^2 + \dot{q}_c^2} \quad (53)$$

$$\mathcal{M}_{LT}^P = 2\dot{\theta}\frac{d}{d\tau} + \ddot{\theta} + \frac{(V_{qq} - V_{pp})\dot{p}_c\dot{q}_c + 2\mu V_{pq}(\dot{p}_c^2 - \dot{q}_c^2)}{\dot{p}_c^2 + \dot{q}_c^2} \quad (54)$$

$$\mathcal{M}_{TL}^P = -2\dot{\theta}\frac{d}{d\tau} - \ddot{\theta} + \frac{(V_{qq} - V_{pp})\dot{p}_c\dot{q}_c + 2\mu V_{pq}(\dot{p}_c^2 - \dot{q}_c^2)}{\dot{p}_c^2 + \dot{q}_c^2} \quad (55)$$

Given the complexity, it is natural to seek a perturbative expansion of the operators. The moving frame rotation angle is set by  $\theta = \tan^{-1} \dot{q}_c/\dot{p}_c \sim O(\mu)$ . From the previous section the edge solution is  $p_c \approx \tanh \tau/2$  and  $q_c \approx -1 + \mu q_1$ . Hence, up to  $O(\mu)$ ,

$$\mathcal{M}_L^P = -\frac{d^2}{d\tau^2} + 1 - \frac{3}{2}\text{sech}^2\frac{\tau}{2} \quad (56)$$

$$\mathcal{M}_T^P = -\frac{d^2}{d\tau^2} + 1 - \mu \left( \text{sech}^2\frac{\tau}{2} + 3q_1 \right) \quad (57)$$

$$\mathcal{M}_{LT}^P = 2\dot{\theta}\frac{d}{d\tau} + \ddot{\theta} + 3\mu\dot{q}_1 \quad (58)$$

$$\mathcal{M}_{TL}^P = -2\dot{\theta}\frac{d}{d\tau} - \ddot{\theta} + 3\mu\dot{q}_1. \quad (59)$$

If the spectrum of  $\mathcal{M}_{rot}^P$  is to be considered only up to  $O(\mu)$  then it is effectively diagonal and we may set  $\mathcal{M}_{TL}^P \times \mathcal{M}_{LT}^P \approx 0$ . Whereas the longitudinal operator is almost exactly that discussed for the diagonal case, we need to examine the spectrum of  $\mathcal{M}_T^P$ . The function  $\text{sech}^2\tau/2 + 3q_1(\tau)$  is negative for all  $\tau$ . In leading order, the lowest eigenvalue of  $\mathcal{M}_T^P$  works out to  $1 - 16\mu^2$ . For this to be positive, and hence the operator to be stable against arbitrary small perturbations, puts the limit  $|\mu| < 1/4$ . The complexity of  $\mathcal{M}_{rot}^P$  suggests that moving to the next order in  $\mu$  will be challenging. Fortunately we can ignore off-diagonal terms since they contribute at  $O(\mu^2)$ ; the full determinant is then simply product of the longitudinal and transverse operators.

We now turn to a discussion of the pre-factor where this will enter crucially.

## VII. FEYNMAN AMPLITUDES

The Gelfand-Yaglom theorem ref.<sup>16</sup> is ideally suited for finding the ratio of determinants that we shall need in the evaluation of the Feynman amplitude for transitions between

potential minima. For a review of calculating functional determinants in QFT see refs.<sup>17,18</sup>. The GY theorem states that for an operator on the interval  $[-T, T]$  with Dirichlet boundary conditions, the ratio of determinants can be calculated from an asymptotic limit:

$$R(\lambda) = \frac{\det \hat{\mathcal{O}}}{\det \hat{\mathcal{O}}_0} = \lim_{T \rightarrow \infty} \frac{\phi(T, \lambda)}{\phi_0(T, \lambda)}. \quad (60)$$

This will now be applied to both the diagonal and edge cases.

### A. Diagonal Motion

First consider the operator describing longitudinal fluctuations for the longitudinal operator  $\mathcal{M}_L^T$ . With  $x = \omega_+ \tau / 2$  this becomes exactly the standard Pöschl-Teller operator:

$$\mathcal{O} = -\frac{d^2}{dx^2} + \kappa^2 - j(j+1)\text{sech}^2 x. \quad (61)$$

A comparison with Eq. 50 yields the asymptotic mass parameter  $\kappa^2 = 4$  and the potential depth  $j(j+1) = 6$ . Pursuing the GY route, the determinant of a Pöschl-Teller operator relative to its free counterpart  $\mathcal{O}_0 = -\frac{d^2}{dx^2} + \kappa^2$  is determined by the transmission amplitude and is exactly expressible as a ratio of Gamma functions:

$$\frac{\det \mathcal{O}}{\det \mathcal{O}_0} = \frac{\Gamma(\kappa)\Gamma(\kappa+1)}{\Gamma(\kappa-j)\Gamma(\kappa+j+1)} \quad (62)$$

However, with  $\kappa = j = 2$ , the above evaluates to zero, reflecting the existence of the translational zero mode. To compute the primed determinant  $\det' \tilde{\mathcal{O}}$ , we must remove this by introducing an infrared regulator  $\epsilon$  that shifts the eigenvalue spectrum:

$$D(\lambda) = \frac{\det(\mathcal{O} - \epsilon)}{\det(\mathcal{O}_0 - \epsilon)}.$$

Computing the small  $\epsilon$  limit gives the normalized primed determinant:

$$\frac{\det' \mathcal{O}}{\det \mathcal{O}_0} = \frac{1}{48}.$$

Restoring the physical dimensions (because one eigenvalue was omitted), gives the final answer for the primed determinant:

$$\chi_L^R(\mu) = \frac{\det \mathcal{M}_{0L}^R}{\det' \mathcal{M}_L^R} = 12\omega_+^2. \quad (63)$$

For the transverse operator the corresponding ratio is,

$$\chi_T^R(\mu) = \frac{\det \mathcal{M}_{0T}^R}{\det \mathcal{M}_T^R} = \frac{\Gamma(\kappa - \ell)\Gamma(\kappa + \ell + 1)}{\Gamma(\kappa)\Gamma(\kappa + 1)}, \quad (64)$$

where  $\kappa, \ell$  are functions of  $\mu$ ,

$$\kappa^2 = \frac{4(1 - 2\mu)}{1 + 2\mu}, \quad \ell(\ell + 1) = \frac{6 - 4\mu}{1 + 2\mu}. \quad (65)$$

All ingredients are now in hand and we may use the general formula for the amplitude  $\mathcal{A}$  derived in Appendix A,

$$\mathcal{A} = T \sqrt{\frac{S_0}{2\pi}} e^{-S_0} \sqrt{\frac{\det A_H^{-1} \mathcal{M}_{rot}}{\det' A^{-1} \mathcal{M}_{rot}}}.$$

For the diagonal path  $p = q$  the result is compactly expressed as,

$$\mathcal{A}_R = CK_R T. \quad (66)$$

Here  $C$  is the free vacuum amplitude and  $K_R$  contains the instanton physics (action and fluctuations):

$$\begin{aligned} C &= \frac{\lambda \sqrt{\omega_+ \omega_-}}{\pi} \exp \left[ -\frac{1}{2}(\omega_+ + \omega_-)T \right] \\ K_R &= \sqrt{\chi_T^R(\mu)} \sqrt{\frac{6S_0^R}{\pi}} e^{-S_0^R} \omega_+ \text{ where,} \\ S_0^R &= \frac{4}{3} \lambda \omega_+, \quad \omega_{\pm} = \sqrt{1 \pm 2\mu}. \end{aligned} \quad (67)$$

Let us now reflect upon the qualitative behavior of  $\chi_T(\mu)$  which is plotted in Fig. 5. Its divergences will be discussed below.

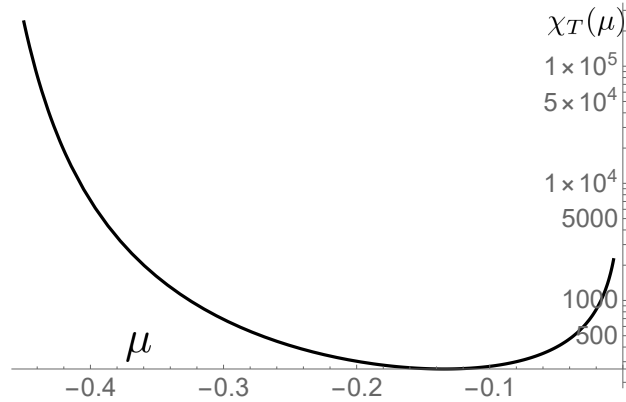


FIG. 5. The ratio of determinants  $\chi_T(\mu)$  as a function of the coupling constant  $\mu$ . The divergence as  $\mu \rightarrow 0$  indicates the presence of an additional zero mode in the uncoupled limit, while the behavior near  $\mu = -0.5$  signals the  $D_4 \rightarrow O(2)$  symmetry melting transition.

For  $\mu = 0$  we have  $\kappa = \ell = 2$  and hence from Eq. 64  $\chi_T(0) \sim \Gamma(0)$  which is infinite. This means that the uncoupled fields are, as expected, free to move both longitudinally and transversely, i.e. there are two zero modes. Expanding near  $\mu = 0$  gives  $\chi_T(\mu) \sim -15/\mu$ . For the amplitude to be real,  $\mu$  must therefore be negative, i.e. the potential between  $p, q$  must be attractive for them to travel together on a diagonal path. The behavior as  $\mu \rightarrow -1/2^+$  is even more intriguing. If we take  $\epsilon = \mu + 1/2$  then  $\kappa = 2/\sqrt{\epsilon} - \sqrt{\epsilon}$  while  $\ell = 2/\sqrt{\epsilon} - 1/2$ . After some further analysis, and use of Stirling's formula, one concludes that an essential singularity exists at  $\mu = -1/2$ :

$$\chi_T \sim \exp\left(\frac{4 \ln 2}{\sqrt{\epsilon}}\right).$$

The physical cause can be understood by inspecting the potential: as  $\mu$  approaches  $-0.5$ , the diagonal barrier vanishes,  $\omega_+ \rightarrow 0$ . The discrete  $D_4$  spatial symmetry has melted into a continuous  $\mathcal{O}(2)$  rotational symmetry. This unphysical divergence of the diagonal amplitude signifies a phase transition from discrete quantum tunneling to continuous zero-point rotation.

## B. Edge Motion

Consider next the operator describing longitudinal and transverse fluctuations for the edge instanton  $\mathcal{M}_L^P$  and  $\mathcal{M}_T^P$ . Following the procedure used for the diagonal instanton we find,

$$\chi_L^P(\mu) = \frac{\det \mathcal{M}_{0L}^P}{\det' \mathcal{M}_L^P} = 12, \quad \chi_T^P(\mu) = \frac{\det \mathcal{M}_{0T}^P}{\det' \mathcal{M}_T^P} = e^{-4\mu} \approx 1 - 4\mu. \quad (68)$$

In analogy with the diagonal case Eq. 67 this yields the final amplitude for the  $P$  instanton,

$$\mathcal{A}_P = CK_P T, \quad K_P = (1 - 2\mu) \sqrt{\frac{6S_0^P}{\pi}} e^{-S_0^P}, \quad S_0^P = \frac{2}{3} \lambda \omega (1 - 2(\pi^2 - 9)\mu^2). \quad (69)$$

Since we have taken equal masses and frequencies for  $p$  and  $q$ ,  $\mathcal{A}_Q = \mathcal{A}_P$  and  $K_Q = K_P$ .

## VIII. DILUTE 3-FLAVOR GAS

In the limit  $T \rightarrow \infty$  the contribution of a single instanton to  $\mathcal{A}$  vanishes because  $T e^{-T} \rightarrow 0$  as  $T \rightarrow \infty$ . The classical EOMs admit solutions beyond those considered so far. For one,

reversing  $t$  gives the anti-instanton of that flavor. For another, any number of well separated instantons and anti-instantons is also a solution if it satisfies the boundary conditions. Extending from the single flavor dilute gas model to three flavors is now our goal.

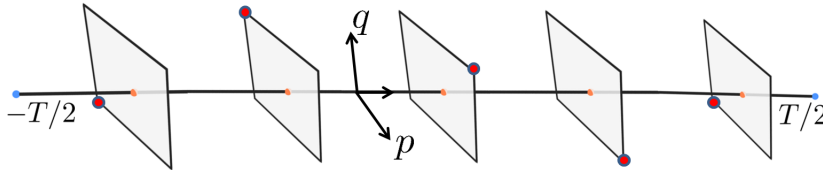


FIG. 6. A chain of 2 DOF instantons as they journey from start to end. The edges of a square are the equilibrium points  $(p, q) = (\pm 1, \pm 1)$ . Each slice has a small but finite thickness corresponding to the instanton width.

The semi-classical prescription requires that one obtain all multi-instanton solutions of the classical EOM's which satisfy the BC's and add up the corresponding amplitudes. A typical multi-instanton configuration has been picturized in Fig. 6. If the number of  $P, Q, R$  instantons is  $N = n + m + l$  then, for sufficiently well separated instantons, the classical action is additive,  $S_0 = nS_0^P + mS_0^Q + lS_0^R$  and the number of possible combinations is,

$$\frac{N!}{n! m! l!}. \quad (70)$$

This fully takes care of the purely classical part of the action - no functional integral had to be performed here.

The quadratic fluctuations need more thought. Let  $\mathbf{U} = \{U_1, \dots, U_N\}$  be the disjoint, time ordered collection of  $N$  time intervals, each interval being roughly one instanton wide, i.e. where  $p^2, q^2$  differ substantially from one. Then the complement  $\bar{\mathbf{U}}$  is the union of those intervals where  $p^2 \approx q^2 \approx 1$ , i.e. where the time evolution occurs via the SHO Hamiltonian for the  $p, q$  DOF's. Obviously  $\mathbf{U} \cup \bar{\mathbf{U}} = [-T/2, T/2]$ .

The dilute gas approximation assumes that a vast distance separates one energy packet from the next and that, correspondingly, the fluctuations around one instanton cannot have any effect on the other. The action Eq. 4 is symmetric under  $p \rightleftharpoons -p$  and  $q \rightleftharpoons -q$ , and so the transition amplitude from any one initial vertex in the  $p - q$  plane to any other vertex (within the same time slice) is independent of the particular starting vertex. This means we can limit our attention to any one chosen vertex and consider horizontal, vertical, and diagonal transitions to the other three vertices (Fig. 7).

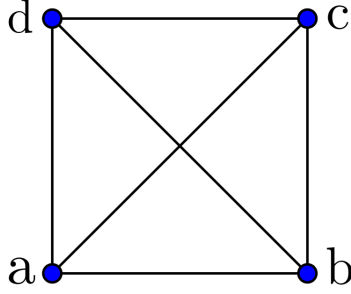


FIG. 7. Horizontal, vertical, and diagonal transitions correspond to P,Q,R instantons. In graph theoretic language this is known as a  $K_4$  graph. Our goal is to derive the transition amplitude between vertices.

Let  $P_i, P_f$  be column/row vectors corresponding to the initial and final states respectively and  $\mathbb{K}$  be the matrix below,

$$\mathbb{K} = \begin{bmatrix} 0 & K_Q & K_R & K_P \\ K_Q & 0 & K_P & K_R \\ K_R & K_P & 0 & K_Q \\ K_P & K_R & K_Q & 0 \end{bmatrix}. \quad (71)$$

In the language of graph theory this is the weighted adjacency matrix of the graph  $K_4$  (fully connected with four vertices and six edges). The element  $K_{ij}$  is the term contributed by the single instanton that connects minimum  $i$  to minimum  $j$ . As an example choose  $P_i = (1 \ 0 \ 0 \ 0)$ ,  $P_f = (0 \ 1 \ 0 \ 0)^T$  for which  $P_f^T \mathbb{K} P_i = K_Q$ . The complete amplitude matrix can be constructed from the basic quantum mechanical rule of multiplying together amplitudes along a particular path. So, at the next time instant, i.e. when the second instanton “fires”, the amplitude in Eq. 71 will be multiplied by  $\mathbb{K}$  until the  $N$ 'th one is reached. In fact  $\mathbb{K}$  is just  $E_0 \mathbb{I} - \mathbb{H}$ , where  $E_0$  is the energy in the absence of tunneling. Each  $\mathbb{K}$  matrix occurs sequentially, i.e. the instantons are time ordered by the identity,

$$\int_{-\frac{T}{2}}^{\frac{T}{2}} \mathbb{K} dt_1 \int_{t_1}^{\frac{T}{2}} \mathbb{K} dt_2 \cdots \int_{t_{N-1}}^{\frac{T}{2}} \mathbb{K} dt_N = \frac{(\mathbb{K}T)^N}{N!}. \quad (72)$$

When the above is summed over all  $N$  we get, of course,  $e^{\mathbb{K}T}$ . Since  $\mathbb{K}$  is a real symmetric matrix with a non-vanishing determinant it can be diagonalized and the amplitude matrix

becomes  $\mathbb{A} = e^{\mathbb{K}T} = S^{-1}e^{\Lambda T}S$  where  $S$  diagonalizes  $\mathbb{K}$ , i.e.  $S^{-1}\mathbb{K}S = \Lambda$  where,

$$\Lambda = \begin{bmatrix} \lambda_S & 0 & 0 & 0 \\ 0 & \lambda_Q & 0 & 0 \\ 0 & 0 & \lambda_P & 0 \\ 0 & 0 & 0 & \lambda_R \end{bmatrix}, \quad S = \frac{1}{2} \begin{bmatrix} 1 & 1 & 1 & 1 \\ -1 & 1 & -1 & 1 \\ -1 & -1 & 1 & 1 \\ 1 & -1 & -1 & 1 \end{bmatrix}. \quad (73)$$

The eigenvalues of  $\mathbb{K}$  are,

$$\lambda_S = K_P + K_Q + K_R, \quad \lambda_Q = -K_P + K_Q - K_R, \quad (74)$$

$$\lambda_P = K_P - K_Q - K_R, \quad \lambda_R = -K_P - K_Q + K_R. \quad (75)$$

That  $\sum \lambda_i = 0$  follows from  $\text{Tr } \mathbb{K} = 0$ . If the vertices of the square, i.e. the minima of the potential, are labeled  $a, b, c, d$  (Fig. 7) then the tunneling amplitudes between them are,

$$\begin{bmatrix} \mathcal{A}_{aa} \\ \mathcal{A}_{ab} \\ \mathcal{A}_{ac} \\ \mathcal{A}_{ad} \end{bmatrix} = C \begin{bmatrix} c_P c_Q c_R + s_P s_Q s_R \\ c_P c_R s_Q + c_Q s_P s_R \\ c_R s_P s_Q + c_P c_Q s_R \\ c_Q c_R s_P + c_P s_Q s_R \end{bmatrix} = \frac{C}{4} \begin{bmatrix} 1 & 1 & 1 & 1 \\ 1 & -1 & 1 & -1 \\ 1 & -1 & -1 & 1 \\ 1 & 1 & -1 & -1 \end{bmatrix} \begin{bmatrix} e^{\lambda_S T} \\ e^{\lambda_P T} \\ e^{\lambda_Q T} \\ e^{\lambda_R T} \end{bmatrix}. \quad (76)$$

In the above we have defined  $c_i \equiv \cosh(K_i T)$  and  $s_i \equiv \sinh(K_i T)$  for  $i \in \{P, Q, R\}$ . By symmetry  $\mathcal{A}_{ad} = \mathcal{A}_{bc}$ ,  $\mathcal{A}_{bd} = \mathcal{A}_{ac}$ ,  $\mathcal{A}_{cd} = \mathcal{A}_{ab}$ . The above result Eq. 76 generalizes the tunneling amplitude in the dilute instanton model for a single DOF to three DOF's.

In order to get a better feel for this result consider the following special cases:

1. **Horizontal/Vertical Instanton:** The  $Q$  instanton (horizontal) corresponds to  $K_P = K_R = 0$ . The only non-zero amplitudes are,

$$\begin{bmatrix} \mathcal{A}_{aa} \\ \mathcal{A}_{ab} \end{bmatrix} = C \begin{bmatrix} \cosh K_Q T \\ \sinh K_Q T \end{bmatrix}. \quad (77)$$

The vertical case is identical, with the  $Q$  label exchanged for  $P$ .

2. **Diagonal Instanton:** For this case  $K_P = K_Q = 0$  and the only non-zero amplitudes are,

$$\begin{bmatrix} \mathcal{A}_{aa} \\ \mathcal{A}_{ac} \end{bmatrix} = C \begin{bmatrix} \cosh K_R T \\ \sinh K_R T \end{bmatrix}. \quad (78)$$

3. **Equal Edge Instantons:** For  $p, q$  fields with identical parameters  $K_P = K_Q = K$  and  $K_R = 0$ , all amplitudes are non-vanishing:

$$\begin{bmatrix} \mathcal{A}_{aa} \\ \mathcal{A}_{ab} \\ \mathcal{A}_{ac} \\ \mathcal{A}_{ad} \end{bmatrix} = C \begin{bmatrix} \cosh^2 KT \\ \frac{1}{2} \sinh 2KT \\ \sinh^2 KT \\ \frac{1}{2} \sinh 2KT \end{bmatrix}. \quad (79)$$

## IX. GAP ENERGIES AND TUNNELING

If the barrier around each of the four wells was infinitely high, a particle would forever remain confined within that well and there would be a four-fold degeneracy. In the semi-classical limit, this degeneracy is lifted by tunneling events. Since our system has  $Z_2 \times Z_2$  symmetry with four degenerate classical vacua  $|a\rangle, |b\rangle, |c\rangle$ , and  $|d\rangle$ , the transition amplitudes calculated via the Euclidean path integral over a large time  $T$  contain the complete information regarding the energy spectrum. The Euclidean evolution operator  $e^{-HT}$  acting on states projects out all higher excited states. As  $T \rightarrow \infty$ , terms scaling as  $e^{-E_n T}$  for  $n \geq 1$  vanish relative to the ground state. This rigorously isolates the finite  $4 \times 4$  subspace of the nearly degenerate ground states localized in the minima. Eigenstates of the Hamiltonian are the following parity-adapted combinations:

$$\begin{aligned} |\psi_S\rangle &= \frac{1}{2} \left[ |a\rangle + |b\rangle + |c\rangle + |d\rangle \right], & |\psi_Q\rangle &= \frac{1}{2} \left[ |a\rangle - |b\rangle - |c\rangle + |d\rangle \right], \\ |\psi_P\rangle &= \frac{1}{2} \left[ |a\rangle + |b\rangle - |c\rangle - |d\rangle \right], & |\psi_R\rangle &= \frac{1}{2} \left[ |a\rangle - |b\rangle + |c\rangle - |d\rangle \right]. \end{aligned} \quad (80)$$

The corresponding energies are  $E_S = -\lambda_S, E_Q = -\lambda_Q, E_P = -\lambda_P, E_R = -\lambda_R$ . Since we have specialized to the identical parameters case  $K_P = K_Q = K$ , there are only two energy gaps as measured from the lowest (symmetric) state,

$$\begin{aligned} \Delta E_P &= \Delta E_Q = E_P - E_S = 2(K + K_R) \\ \Delta E_R &= E_R - E_S = 4K. \end{aligned}$$

The above theoretical splittings can be compared against the near-exact four energies numerically calculated for negative  $\mu$  by solving the Schrodinger partial differential equation on a grid. The semi-classical and quantum splittings should converge as the effective Planck

constant gets smaller. In Fig. 8 one indeed sees that this is true, affirming the correctness of our approximations. Recall that although the calculation for  $K_R$  was exact, that for the action in  $K$  was correct to  $O(\mu^2)$  and in the pre-factor to  $O(\mu)$ .

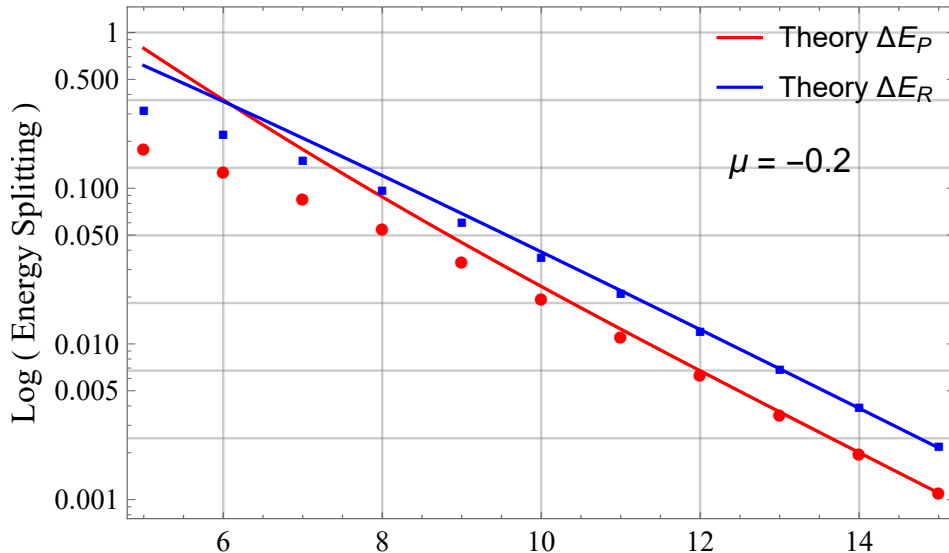


FIG. 8. Semi-classical instanton results compared with high-precision numerical diagonalization for the ground-state energy splittings as a function of the effective inverse Planck constant  $\lambda$  for the case of attractive coupling ( $\mu = -0.2$ ), where the diagonal  $R$  path is energetically competitive.

The results in the two figures are for a middle value;  $\mu = \mp 0.2$ . Since our treatment of the edge instantons is perturbative,  $|\mu|$  cannot be allowed to be too large. Whereas the diagonal instanton's  $K_R$  should totally dominate the edge instanton's  $K$  near  $\mu = -0.5$ , this region is numerically inaccessible because  $\lambda$  must become extremely large for the semi-classical approximation to be valid but in this case the splittings become so small that infinite precision arithmetic is needed for solving the partial differential equation. For a repulsive potential (positive  $\mu$ ) as in Fig. 9, the  $p, q$  fields travel separately.  $K_R$  is effectively zero and so  $\Delta E_R = 2\Delta E_P = 4K$ .

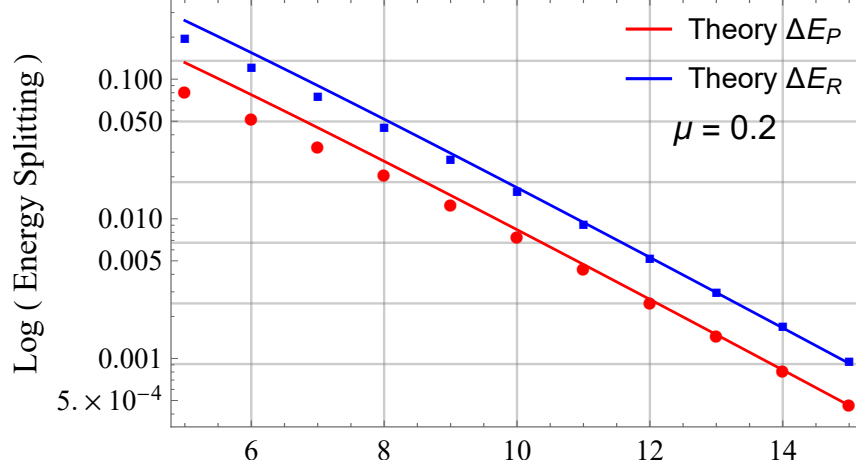


FIG. 9. As in Fig.8 but for repulsive coupling (positive  $\mu$ ),  $\mu = 0.2$ . Tunneling is dominated by the edge-path configurations.

To analyze the real-time dynamics, we perform a Wick rotation  $\tau \rightarrow it$ . The overall normalization constant  $C$  drops out when calculating normalized probabilities, as the zero-point energy transforms into an unobservable global phase  $e^{-iE_0t}$ . Suppose that at  $t = 0$  the system is prepared entirely in the  $a$  well, i.e. in  $|a\rangle = |-1, -1\rangle$ . Thereafter the state evolves unitarily as  $|\psi(t)\rangle = e^{-iHt} |a\rangle$ . We can factor out the common global phase  $e^{-iE_0t/\hbar}$ , which vanishes when calculating probabilities. Thus the probability of remaining in well  $a$  is,

$$P_a(t) = \frac{1}{4} [1 + \cos^2 2Kt + 2 \cos 2Kt \cos 2K_R t]. \quad (81)$$

To find the characteristic tunneling lifetime out of the initial minimum, we examine the short-time depletion rate:

$$P_a(t) = 1 - (2K^2 + K_R^2)t^2 + \mathcal{O}(t^4). \quad (82)$$

Consequently, the characteristic lifetime  $\tau$  is:

$$\tau = \frac{\pi}{2\sqrt{(2K^2 + K_R^2)}}. \quad (83)$$

The probability of transitioning from  $a$  to adjacent minima  $b$  or  $d$  is,

$$P_b(t) = P_d(t) = \frac{1}{4} \sin^2 2Kt. \quad (84)$$

Finally, the probability of transitioning from  $a$  to the diagonal minimum  $c$  is,

$$P_c(t) = \frac{1}{4} [1 + \cos^2 2Kt - 2 \cos 2Kt \cos 2K_R t]. \quad (85)$$

The dynamics reveal that tunneling to adjacent wells ( $b, d$ ) is governed exclusively by the parameter  $K$ , while the probabilities of remaining in  $a$  or tunneling diagonally to  $c$  exhibit a beat frequency driven by the interplay between the orthogonal instanton paths  $K$  and  $K_R$ .

## X. COMPARISON WITH OTHER APPROACHES

Although instanton theory has found some application to neural networks and biological systems, the most robust and prolific application of multi-dimensional instanton theory to potentials with four or more minima is found in chemical physics. In these systems, the degrees of freedom represent nuclear coordinates and, after using the Born-Oppenheimer approximation, the computed potential energy surfaces inherently feature multiple symmetric and asymmetric minima connected by complex saddle points. In the following we shall confine our attention to molecular dynamics.

Richardson’s RPI theory<sup>1-3</sup> is primarily designed as a computational workhorse for calculating thermal reaction rates and tunneling splittings in high-dimensional molecular systems. It relies on discretizing the imaginary-time path integral into a “ring polymer” consisting of  $N$  beads. In this discrete space, the zero mode emerges as a zero-frequency eigenvalue in the mass-weighted ring-polymer Hessian matrix (corresponding to the cyclic permutation of the beads along the imaginary-time loop). Instead of the Jacobian that emerges in the continuum (as in the foundational papers<sup>10-12</sup> of the 1980’s and in our paper), Richardson et. al. handle this by simply excluding this zero eigenvalue from the steepest-descent product and replace it with an integration over the imaginary time. Further, rather than sum over an infinite series of instanton terms, standard RPI is typically formulated for a single barrier crossing event to calculate thermal reaction rates, i.e. it seeks the single optimal tunneling pathway—a first-order saddle point on the extended ring-polymer potential energy surface. Ring Polymer Molecular Dynamics<sup>4</sup> (RPMD) further develops RPI for simulating multidimensional tunneling. Quantum fluctuations are statistically sampled without ever calculating an exact pre-factor, a direct contrast with our paper where this is a central concern. While this work relies on the continuous-time Gelfand-Yaglom method to exact the functional determinants, computational approaches to multidimensional instanton theory take a very different approach. In their calculation of reaction rate constants, Lohle and Kästner<sup>5</sup> compute the fluctuation pre-factor by diagonalizing massive Hessian matri-

ces derived from the discretized path, bypassing the explicit separation of longitudinal and transverse modes. Furthermore, while this numerical approach observes the breakdown of semiclassical instanton theory via the spatial collapse of the trajectory at a crossover temperature, our analytical approach identifies this breakdown explicitly as an essential singularity in the pre-factor, corresponding to the  $D_4 \rightarrow O(2)$  symmetry melting.

Kryvohuz<sup>6</sup> realizes, as we do, the necessity of separating the “soft” tunneling direction from the transverse vibrational modes. He also introduces a local orthogonal coordinate system moving along the instanton path to isolate the longitudinal reaction coordinate. However, rather than analytically projecting it out via Faddeev-Popov and Gelfand-Yaglom, he treats the transverse degrees of freedom using a steepest descent approximation and numerically integrates out the orthogonal coordinates by evolving a stability matrix (which he denotes as  $R_{2N-2}$ ) along the instanton trajectory. He does not sum over multiple topological instanton types in a dilute gas framework because his method is designed for chemical reactions escaping a metastable well (e.g., passing over a single saddle point from reactants to products, like  $H + H_2 \rightarrow H_2 + H$ ). He assumes a single tunneling channel and does not build a coherent superposition of multi-flavor pathways. Consequently, his algorithm searches only for the dominant periodic instanton trajectory (the minimum action path).

Eraković et. al.<sup>7</sup> develop a multidimensional semiclassical instanton theory to calculate ground-state tunneling splittings in asymmetric (biased) quartic potentials. They bypass calculating and diagonalizing a massive fluctuation matrix as is typically done in the standard RPI method. Instead they handle the fluctuations—and effectively the zero mode—by integrating a Riccati differential equation along the characteristic instanton path. The string method is used to numerically locate the instantons. They do not perform infinite dilute gas summations analytically, as we do. Instead, to compute the tunneling splitting patterns of a cluster, they identify the Minimum Action Paths (MAPs) connecting adjacent symmetry-equivalent wells.

Benderskii et. al.<sup>8</sup> use a potential that can be directly mapped into ours (Eq.4) but do not explicitly project out the zero mode. Instead they approach the problem through the lens of trajectory stability and look at the lowest eigenvalue (which they term the stability parameter  $\Lambda$ ) of the second functional derivative of the action with respect to trajectory variations. The  $P, Q, R$  instantons in our paper can be readily identified with the same paths in their paper. However, their analysis restricts itself to evaluating the competition

between these trajectories for a single tunneling event across the barrier to find the crossover behavior of the splitting  $\Delta_0$ . They do not string multiple, distinct instanton events together into a time-ordered sequence to construct a multi-state transition amplitude matrix.

## XI. SUMMARY

In adding an extra DOF to the canonical single DOF instanton problem, significant new issues and new phenomena are encountered. First, to find the classical path requires solving coupled Euler-Lagrange equations. These are non-linear differential equations that generally do not admit exact solutions. One can always hope that by using some clever transformation an exact solution can be achieved. While it is still possible to solve them numerically, fortunately the choice of equal system parameters for both systems allowed symmetry considerations to guide us to an exact solution for the diagonal instanton. Surprisingly it turned out that diagonal travel has lower action compared to edge travel but this is true only for highly attractive coupling between fields.

For weak coupling we found excellent agreement between the calculated semi-classical energy splittings and the “exact” solution of the Schrodinger equation, i.e. a numerical solution using a sufficiently fine grid. This holds true for even rather large  $|\mu|$  values, i.e. close to the validity limit of  $|\mu| = 0.25$ . This convergence fails as the symmetry melts. Near  $\mu = -0.5$ , the splittings become so small that they require infinite-precision arithmetic to resolve numerically.

As the coupling parameter  $\mu$  approaches the critical value of  $-0.5$ , the potential barrier along the diagonal path vanishes entirely. The four discrete, degenerate minima at  $(\pm 1, \pm 1)$  dissolve, and the system forms a continuous circular “Mexican-hat” valley. This transformation creates a continuous moduli space where the ground state is no longer localized in discrete wells but resides in a continuous manifold of zero-point rotation. The discrete  $D_4$  spatial symmetry of the four-well system dissolves in to a continuous  $\mathcal{O}(2)$  rotational symmetry. This phenomenon, which we term “symmetry melting,” has several critical theoretical implications.

First, in usual tunneling calculations the rate is dominated by  $e^{-S/\hbar}$  while the prefactor plays a subsidiary role. But, as we saw here for the quartic potential, the semiclassical approximation breaks down as  $\mu \rightarrow -1/2$ . This is signalled by the unphysical divergence

of the transverse fluctuation prefactor  $\chi_T(\mu)$ . This serves as a mathematical “red flag” for the limits of our model. Specifically, the essential singularity  $\chi_T \sim \exp(4 \ln 2/\sqrt{\epsilon})$  indicates that in this regime, tunneling between isolated vacua is replaced by free rotation, meaning the concept of a single “tunneling event” between discrete states loses its physical meaning. This suggests a phase transition where isolated discrete quantum tunneling is replaced by free continuous zero-point rotation in the ground state manifold.

In calculating the pre-factor, to be on the side of caution, we used the Faddeev-Popov procedure in field theory as adapted to the quantum mechanical situation by Zinn-Justin. For the 1-D case it leads to exactly the same Jacobian factor as the more conventional treatment. However it gives reassurance that no change is required when more than one field is present with the proviso that the single instanton action be replaced by the sum of actions (instanton-lump or instanton-instanton).

Summing over instanton paths with three different types is another result achieved in this work. A single instanton makes a vanishingly small contribution to the amplitude, a fact that made necessary the dilute instanton gas model for a single DOF. There an infinite number of time sequenced instantons is summed over to give a finite contribution to the amplitude. This is true here as well except that the paths are far more complex because there are two edge instantons and a diagonal one as well. This is picturized in Fig. 6. Each slice can be placed anywhere in the (nearly) infinitely long time axis without any change of action. Following the usual quantum mechanical rule for compounding amplitudes, and drawing inspiration from graph-theoretic networking, we arrived at a closed form analytical expression for tunneling from any vertex to any other. This allows for probabilities to slosh between minima at a calculable rate, i.e. to a modified Rabi frequency.

While the physical model for composite tunneling (Appendix B) was the initial motivation for a mathematical exploration of the model considered here, one hopes that other physical systems exist where the present formalism will also have relevance. Beyond the example considered here, there are likely to be other systems where synchronous tunneling may be relevant. These could include a two dimensional free electron gas subjected to a perpendicular, spatially varying magnetic field. Electrons move along snake-like classical paths on either side of the line where the field crosses zero. This system of spinless electrons is described quantum mechanically by a symmetric double well potential<sup>19</sup>. Were one to take into account the electron’s magnetic moment as well, the resulting effective action is

similar to Eq. 4. Suitably designed optical lattices might provide yet other opportunities.

## Appendix A: Faddeev-Popov Procedure

For a single DOF instanton textbooks give the standard method for extracting the Jacobian associated with the zero mode. On the other hand the Faddeev-Popov procedure, which was applied to the single DOF case by Zinn-Justin<sup>15</sup>, extends directly to the present case of multiple DOF's. To be on the safe side, we chose to go the rigorous way using this method rather than assume that the canonical way holds in the present case.

The starting point is the identity,

$$\frac{1}{\sqrt{2\pi\beta}} \int_{-\infty}^{\infty} d\lambda e^{-\frac{\lambda^2}{2\beta}} = 1, \quad (\text{A1})$$

For the problem at hand, we make the following particular choice for  $\lambda$ :

$$\lambda(t^*) = \int dt \dot{\Phi}_c^T(t) A[\Phi(t+t^*) - \Phi_c(t)]. \quad (\text{A2})$$

Here  $t^*$  is chosen arbitrarily with the intent of breaking the invariance of the action under time translations. The arbitrary parameter  $\beta$  will eventually disappear from the final result for  $\mathcal{A}$ . The above expression is then inserted into the amplitude

$$\mathcal{A} = \mathcal{N} \int [d\Phi] e^{-S[\Phi]} \times \frac{1}{\sqrt{2\pi\beta}} \int_{-\infty}^{\infty} dt^* \frac{d\lambda}{dt^*} e^{-\frac{\lambda^2}{2\beta}}. \quad (\text{A3})$$

Next, the integration variable is changed from  $\Phi(t)$  to  $R(t) = \Phi(t+t^*)$  and then back to  $\Phi(t)$  making the integrand independent of  $t^*$ . After these manipulations the amplitude becomes,

$$\mathcal{A} = \mathcal{N} \int [d\Phi] \int \frac{dt^* dt}{\sqrt{2\pi\beta}} \dot{\Phi}_c^T(t) A \dot{\Phi}(t) e^{-S_\beta[\Phi]},$$

where,  $S_\beta \equiv S + \frac{\lambda^2}{2\beta} = S + \frac{1}{2\beta} \left[ \int dt \dot{\Phi}_c^T(t) A[\Phi(t) - \Phi_c(t)] \right]^2$ .

Since the second term above is positive definite, the effective action  $S_\beta$  is obviously minimized, as was the original action  $S$ , at  $\Phi = \Phi_c$ . This leaves the EOM's unchanged and eliminates the linear term. The  $t^*$  integral extends over the entire domain  $[-T/2, T/2]$  and is trivial. Thus,

$$\mathcal{A} = \frac{\mathcal{N}T}{\sqrt{2\pi\beta}} \int [d\Phi] \int dt \dot{\Phi}_c^T(t) A \dot{\Phi}_c(t) e^{-S_\beta[\Phi]}. \quad (\text{A4})$$

At this point the  $\Phi$  integration is replaced by integration over the set of basis coefficients  $\alpha_n$  with  $n = 0, 1, 2 \dots$ .

$$\Omega(t) = \sum_{n=0} \alpha_n \Phi_n(t), \quad [d\Phi] = \frac{d\alpha_0}{\sqrt{2\pi}} [d\alpha]', \quad \text{where, } [d\alpha]' \equiv \prod_{n=1}^{\infty} \frac{d\alpha_n}{\sqrt{2\pi}}. \quad (\text{A5})$$

The boundary conditions at  $\pm T/2$  ensure that,

$$\int dt \dot{\Phi}_c^T(t) A \Phi_c(t) = 0 \quad (\text{A6})$$

so that, after using Eq. A2, the parameter  $\lambda(0)$  can be rewritten as  $\sqrt{S_0}\alpha_0$ . Performing the  $\alpha_0$  integral then yields,

$$\mathcal{A} = \mathcal{N} \frac{T}{\sqrt{2\pi}} e^{-S_0} \sqrt{S_0} \int [d\alpha]' e^{-S_2}, \quad (\text{A7})$$

where the zero mode has been integrated out and the integration is now to be done over the quadratic level fluctuations. In the functional integration one may equally well integrate over fields in the lab fixed frame or the rotating frame. In the latter case the quadratic level part takes the form,

$$\frac{1}{2} \int dt \tilde{\Phi}^T \mathcal{M}_{rot} \tilde{\Phi}. \quad (\text{A8})$$

Denoting the eigenvalues of  $A^{-1} \mathcal{M}_{rot}$  by  $\lambda_n$ , we can now complete the formal analysis:

$$S_2 = \frac{1}{2} \sum_{n=0} \lambda_n \alpha_n^2. \quad (\text{A9})$$

and so the remaining integral is,

$$\int [d\alpha]' e^{-S_2} = \prod_{n \neq 0} \frac{1}{\sqrt{\lambda_n}} \equiv \frac{1}{\sqrt{\det' A^{-1} \mathcal{M}_{rot}}}. \quad (\text{A10})$$

(The  $A^{-1}$  simply takes away the  $a_p, a_q$  factors). For any classically defined path stable against transverse perturbations, the amplitude is,

$$\mathcal{A} = \frac{T}{\sqrt{2\pi}} e^{-S_0} \sqrt{S_0} \frac{\mathcal{N}}{\sqrt{\det' A^{-1} \mathcal{M}_{rot}}}. \quad (\text{A11})$$

To complete the calculation we must determine  $\mathcal{N}$ . This will be done by taking the ratio with the harmonic oscillator determinant - in this case that for two coupled oscillators. With reference to Fig.1, let us consider the amplitude for a path that starts and returns from any one of the potential minima ( $\pm 1, \pm 1$ ) where the potential is nearly harmonic. In that case the semiclassical approximation to the amplitude gives,

$$\mathcal{N} \int [dpdq] e^{-S_2} = \frac{\mathcal{N}}{\sqrt{\det A^{-1} \mathcal{M}^H}}, \quad (\text{A12})$$

Because it has only quadratic terms, the matrix  $\det A^{-1}\mathcal{M}^H$  can be diagonalized and its determinant evaluated. The shifted frequencies are,

$$\omega_{\pm}^2 = \frac{1}{2}(\omega_p^2 + \omega_q^2) \pm \frac{1}{2}\sqrt{(\omega_p^2 - \omega_q^2)^2 + 16\mu\nu\omega_p^2\omega_q^2},$$

and the normalization constant is,

$$\mathcal{N} = \sqrt{\frac{m_p\omega_+}{\pi\hbar}} \sqrt{\frac{m_q\omega_-}{\pi\hbar}} e^{-\frac{1}{2}(\omega_+ + \omega_-)T} \sqrt{\det A^{-1}\mathcal{M}^H} \equiv C\sqrt{\det A^{-1}\mathcal{M}^H}. \quad (\text{A13})$$

$C$  is defined in terms of the two particle harmonic oscillator wavefunction evaluated at the origin,

$$C = |\Psi_0(0, 0)|^2 e^{-\frac{1}{2}(\omega_+ + \omega_-)T}. \quad (\text{A14})$$

Inserting the into Eq. A7 we arrive at the final form of  $\mathcal{A}$ , which is the central result of this section,

$$\mathcal{A} = T\sqrt{\frac{S_0}{2\pi}} e^{-S_0} \sqrt{\frac{\det A_H^{-1}\mathcal{M}_{rot}}{\det' A^{-1}\mathcal{M}_{rot}}}. \quad (\text{A15})$$

## Appendix B: Composite Tunneling

In atomic and nuclear physics the tunneling of a composite system has often been tackled using a coupled channel approach for scattering processes. This seeks to directly solve the time dependent Schrödinger equation and is heavily computational. Though straightforward in principle, little theoretical insight can be gained. Some papers are referenced in the book by Razavy<sup>14</sup>.

Instead, let us consider a system where the tunneling object is finite-sized rather than point-like, i.e. a one-dimensional diatomic “molecule” made of two distinguishable point-like atoms joined by a perfectly rigid rod of length  $L$ . If such a molecule is placed entirely within one well, it will seek to tunnel into the other well much as a point particle would. Let us assume the two atoms experience identical potentials  $U(x)$ , each having the form of a symmetric double well,

$$U(x) = \frac{m\omega^2}{16a^2}(x^2 - a^2)^2. \quad (\text{B1})$$

For simplicity take the atomic masses as equal,  $m_1 = m_2 = \frac{m}{2}$ . The centre of mass  $y = \frac{1}{2}(y_1 + y_2)$  is equidistant from the two constituents and the relative distance  $x = x_1 - x_2$  is

fixed at  $L$ . The (Euclidean) Lagrangian is,

$$\mathcal{L} = \frac{m}{2}\dot{y}^2 + \bar{U}, \quad \bar{U} = U\left(y + \frac{L}{2}\right) + U\left(y - \frac{L}{2}\right) \quad (\text{B2})$$

The potential  $\bar{U}$  is symmetrical under  $y \rightarrow -y$ , i.e. the cm may be located equally within either well. The key observation is that  $\bar{U}$  may be written as a symmetric double well with minima at  $y = \pm y_0$  with  $y_0 \neq a$ .

$$\bar{U} = \frac{m\omega^2}{8a^2} (y^2 - y_0^2)^2 + K, \quad y_0 = \pm af, \quad f = \sqrt{1 - \frac{3L^2}{4a^2}}, \quad K = \frac{m\omega^2 L^2}{8} \left(1 - \frac{L^2}{2a^2}\right). \quad (\text{B3})$$

$K$  is a constant that may be discarded. In the limit  $L \rightarrow 0$ ,  $\bar{U}$  reduces to  $2U$ . The classical EOM following from  $\mathcal{L}$  is,

$$\ddot{y}_c = \frac{\omega^2}{2a^2} (y_c^2 - y_0^2) y_c, \quad (\text{B4})$$

with a modified instanton solution that interpolates between the shifted vacua that are now located at  $\pm y_0$ . Note that for  $L \rightarrow 2a/\sqrt{3}$  the double minimum becomes a pure quartic with a single minimum at  $y_0 = 0$ ,

$$\bar{U} \rightarrow \frac{m\omega^2}{8a^2} y^4 + \frac{1}{18} m\omega^2 a^2. \quad (\text{B5})$$

There is no instanton solution in the above limit. The condition of perfect rigidity can be relaxed by adding a kinetic term for relative motion as well as an extra potential chosen to constrain  $x$  near  $L$ , now to be thought of as the length parameter determining the average length of the vibrating molecule,

$$\mathcal{L} = \frac{m}{2}\dot{y}^2 + \frac{m}{8}\dot{x}^2 + U_T. \quad (\text{B6})$$

In terms of the double well potential  $U$  in Eq. B1 the new potential  $U_T$  is,

$$U_T = U\left(y + \frac{x}{2}\right) + U\left(y - \frac{x}{2}\right) + \frac{m\Omega^2}{32L^2} (x^2 - L^2)^2 \quad (\text{B7})$$

As  $\Omega \rightarrow \infty$  the molecule becomes increasingly rigid with equilibrium points close to  $x = \pm L$ . To proceed further, we find the minima of  $U_T$  and then re-express it with appropriately defined constants,

$$U_T = \frac{m\tilde{\Omega}^2}{32L^2} (x^2 - x_0^2)^2 + \frac{m\omega^2}{8a^2} (y^2 - y_0^2)^2 + \frac{3m\omega^2}{16a^2} (y^2 - y_0^2)(x^2 - x_0^2) + C \quad (\text{B8})$$

The potential minima are at  $x = \pm x_0$ ,  $y = \pm y_0$  where  $x_0, y_0$  and the remaining constants are:

$$x_0^2 = \frac{1 - \frac{2\omega^2}{\Omega^2}}{1 - \frac{2\omega^2 L^2}{\Omega^2 a^2}} L^2, \quad y_0^2 = \frac{1 - \frac{3L^2}{4a^2} - \frac{\omega^2 L^2}{2a^2 \Omega^2}}{1 - \frac{2\omega^2 L^2}{a^2 \Omega^2}} a^2 \quad (\text{B9})$$

$$\tilde{\Omega}^2 = \Omega^2 \left( 1 + \frac{\omega^2 L^2}{4a^2 \Omega^2} \right), \quad C = \frac{1}{8} m \omega^2 L^2 \frac{1 - \frac{\omega^2}{\Omega^2} - \frac{L^2}{2a^2}}{1 - \frac{2L^2 \omega^2}{a^2 \Omega^2}} \quad (\text{B10})$$

The constant  $C = E_{min}$  is irrelevant to the dynamics but has been listed above for completeness. Note that as  $\Omega \rightarrow \infty$  the equilibrium positions shift towards the free values,  $x_0 \rightarrow L, y_0 \rightarrow fa$ .

Non-rigidity allows for molecular vibrations. At the other extreme, one could imagine the atoms to be either totally free or very loosely bound together. In that case, intuitively speaking, one atom may tunnel to the other side sooner than the other resulting in a 180° flip of the molecule’s orientation when eventually both atoms cross over. One expects that the transition probabilities for spin flip and no flip will be equal if both atoms experience exactly the same potential. However if there is some small difference then one would have an asymmetric double well with a single true vacuum and two different transition probabilities. In Eq. B8 we have precisely the form of quartic potential which we sought to explore in this work; the potential  $V(p, q)$  emerged in a very natural way.

## CONFLICT OF INTEREST

The authors have no conflicts to disclose.

## DATA AVAILABILITY STATEMENT

The data that support the findings of this study are available from the corresponding author upon reasonable request.

## REFERENCES

- <sup>1</sup>J. O. Richardson, *Int. Rev. Phys. Chem.* **37**, 171 (2018).
- <sup>2</sup>J. O. Richardson and S. C. Althorpe, *J. Chem. Phys.* **148**, 200901 (2018).
- <sup>3</sup>M. R. Fiechter, G. Laude, and J. O. Richardson, *J. Chem. Phys.* **164**, 024104 (2026).

- <sup>4</sup>S. Habershon, D. E. Manolopoulos, T. E. Markland, and T. F. Miller III, *Annu. Rev. Phys. Chem.* **64**, 387 (2013).
- <sup>5</sup>A. Lohle and J. Kästner, *J. Chem. Theory Comput.* **14**, 5489 (2018).
- <sup>6</sup>M. Kryvohuz, *J. Chem. Phys.* **134**, 114103 (2011).
- <sup>7</sup>M. Eraković, C. L. Vaillant, and M. T. Cvitaš, *J. Chem. Phys.* **152**, 084111 (2020).
- <sup>8</sup>V. A. Benderskii, E. V. Vetoshkin, E. I. Kats, and H. P. Trommsdorff, *Phys. Rev. E* **67**, 026102 (2003).
- <sup>9</sup>S. C. Althorpe, *Eur. Phys. J. B* **94**, 155 (2021).
- <sup>10</sup>V. A. Novikov, M. A. Shifman, A. I. Vainshtein, and V. I. Zakharov, *XVI Winter School of Physics of Leningrad Institute for Nuclear Physics (LNPI, Leningrad, 1981)*.
- <sup>11</sup>S. Coleman, *Aspects of Symmetry: Selected Lectures of Sidney Coleman* (Cambridge University Press, Cambridge, 1985).
- <sup>12</sup>G. 't Hooft, *Phys. Rev. Lett.* **37**, 8 (1976).
- <sup>13</sup>F. Devoto, S. Devoto, L. Di Luzio, and G. Ridolfi, *J. Phys. G: Nucl. Part. Phys.* **49**, 103001 (2022).
- <sup>14</sup>M. Razavy, *Quantum Theory of Tunneling*, 2nd ed. (World Scientific, Singapore, 2014).
- <sup>15</sup>J. Zinn-Justin, *Path Integrals in Quantum Mechanics* (Oxford University Press, Oxford, 2005).
- <sup>16</sup>I. M. Gelfand and A. M. Yaglom, *J. Math. Phys.* **1**, 48 (1960).
- <sup>17</sup>G. V. Dunne, *J. Phys. A: Math. Theor.* **41**, 304006 (2008).
- <sup>18</sup>J. Casahorran, *Fortschr. Phys.* **50**, 405 (2002).
- <sup>19</sup>P. Hoodbhoy, *J. Phys.: Condens. Matter* **30**, 185301 (2018).